

## Antiprismatic Crystal Field and Paramagnetic Susceptibility of $U^{4+}$ Sulfates

J. MULAK

*Institute for Low Temperature and Structure Research, Polish Academy of Sciences, Plac Katedralny 1, P.O.B. 937, 50-950 Wrocław, Poland*

Received November 17, 1977; in revised form February 2, 1978

On the basis of the simplified model of the  $U^{4+}$  ion in a distorted axial crystal field, the temperature dependence of the magnetic susceptibilities of three  $U^{4+}$  sulfates,  $U(SO_4)_2 \cdot 4H_2O$ ,  $U_6O_4(OH)_4(SO_4)_6$ , and  $U(OH)_2SO_4$ , within the temperature range 4.2–300°K has been investigated and interpreted. This model proved to be successful, and the only parameters fitted empirically were the values of the crystal field splitting. The antiprismatic coordination ( $D_{4d}$ ) of the uranium ion in these compounds was confirmed and its electronic ground states were determined. The system of two singlets  $1/2^{1/2}|3\rangle \pm 1/2^{1/2}|-3\rangle$  originating from the doublet  $1 \pm 3$  is the ground state of the uranium ion in  $U(SO_4)_2 \cdot 4H_2O$ . An analogous system of two singlets  $1/2^{1/2}|2\rangle \pm 1/2^{1/2}|-2\rangle$  is the ground state in  $U_6O_4(OH)_4(SO_4)_6$ . For  $U(OH)_2SO_4$ , the doublet  $1 \pm 2$  is the ground state above 21°K, whereas below this temperature it becomes split into the two singlets  $1/2^{1/2}|2\rangle \pm 1/2^{1/2}|-2\rangle$ , probably because of a crystallographic distortion induced by the cooperative Jahn–Teller effect. Deviations from the  $D_{4d}$  symmetry of the uranium ion coordination occurring in these compounds are discussed.

### Introduction

At least three distinct crystalline phases, among them two alkaline salts, were found in the system  $UO_2-SO_3-H_2O$  previously. They are  $U(SO_4)_2 \cdot 4H_2O$ ,  $U_6O_4(OH)_4(SO_4)_6$ , and  $U(OH)_2SO_4$ . Their crystal structures are precisely known from the very reliable determinations carried out by Lundgren (1, 2) and Kierkegaard (3). With respect to the uranium ion sublattice structure, these compounds differ very significantly from each other. The crystal of  $U(SO_4)_2 \cdot 4H_2O$  is built up of layers formed by uranium ions and sulfate groups held together by water molecules. The lattice of  $U_6O_4(OH)_4(SO_4)_6$  is composed of isolated  $[U_6O_4(OH)_4]^{12+}$  groups, whose six uranium ions form an octahedron. The crystal of  $U(OH)_2SO_4$  has a "thready" structure, and the uranium ions linked together by  $OH^-$  ions

form zigzag  $[U(OH_2)]_n^{2n+}$ -chains; the distance between them is about 6 Å.

On the other hand, these three compounds have one common feature: approximately the same antiprismatic coordination of the  $U^{4+}$  ion by oxygen anions with almost identical U–O distances. This feature makes possible an investigation of the influence of low-symmetry distortions of the electrostatic field at the uranium ion on its magnetic susceptibility.

The interpretation of the temperature dependence of the magnetic susceptibility is based on the simplified model of the uranium(4+) ion with the  $^3H_4$  ground term and  $J = 4$  as a good quantum number in the antiprismatic crystal field with regard to the splitting of axial  $1 \pm M_J$  doublets in the first approximation. This model proved to be fully adequate, and the only parameters fitted empirically were the values of the splitting in the crystal field. The

fitting of the parameters to the Van Vleck equation was carried out numerically according to the assumed pattern of the splitting. The calculated splitting values  $\delta$  are optimum with regard to the theoretical values of Zeeman matrix elements, with the latter considered fixed.

Until recently, only the magnetic susceptibility of  $U(SO_4)_2 \cdot 4H_2O$  within the temperature range 4.2–300°K and its approximate interpretation has been given (4).

### Experimental

The saturated solution of  $U^{4+}$  sulfate was the starting material for preparation of all three  $U^{4+}$  sulfates in the crystalline form. Each compound was obtained at fixed, in each case different, parameters of crystallization—pH of the solution, temperature (pressure), and concentration (1–3). All the crystallization processes were performed in thick-walled glass tubes for about 200 hr. Uranium sulfate tetrahydrate was obtained from a saturated solution in 1 *M*  $H_2SO_4$  at 90°C as a green crystalline precipitate, mostly in clusters. The dark green crystals of  $U_6O_4(OH)_4(SO_4)_6$  in the shape of rather thick octagonal or square plates were obtained from the saturated solution of uranium sulfate in 0.5 *M*  $H_2SO_4$  at 200°C.  $U(OH)_2SO_4$  crystallized from the diluted solution (1:1) in 0.3 *M*  $H_2SO_4$  at 140°C in the shape of black rods, often in clusters. The sizes of the crystals were different according to subtle changes in the crystallization parameters.

The identification of the phases was based on X-ray powder diagrams taken with an X-ray diffractometer of the DRON-1.5 type. The range of diffraction angles 5–30° was under control, and in every case no fewer than 30 known, characteristic reflections together with their intensities were identified. The prepared crystals were characterized by high-phase purity (no unidentified reflections were observed) and by homogeneity of crystal shapes and color (microscopic observation). This

means that distinct crystalline phases are formed selectively, according to the conditions. The choice of crystallization parameters proved to be especially important for  $U(OH)_2SO_4$ . If they were not chosen appropriately, either a black precipitation of hydrated uranium dioxide (or  $U(OH)_4$ ) with  $UO_2$  crystal structure or the green crystals of the neutral tetrahydrate were obtained.

Measurements of the paramagnetic susceptibilities of  $U_6O_4(OH)_4(SO_4)_6$  and  $U(OH)_2SO_4$  within the temperature range 4.2–300°K were carried out for the powdered material by the Faraday method at a magnetic field of 5 kOe by means of an electronic Cahn balance with continuous recording of the force acting on the sample as a function of temperature. Samples of about 200 mg of the mass were usually used. In addition, for  $U(OH)_2SO_4$  the dependence of the magnetization on the magnetic field strength in the range 0–50 kOe at 4.2°K, as well as the  $\chi(T)$  dependence over the range 4.2–50°K for 5, 10, 20, 30, 40, and 50 kOe, was measured by means of a Foner vibrating-sample magnetometer of PAR-150A type.

The data on the magnetic susceptibility of  $U(SO_4)_2 \cdot 4H_2O$  are taken from our earlier work (4).

The values of the magnetic susceptibility given in the text and figures are specified in electromagnetic units per mole. Assumed corrections for diamagnetism of  $U(SO_4)_2 \cdot 4H_2O$ ,  $U_6O_4(OH)_4(SO_4)_6$ , and  $U(OH)_2SO_4$  are  $-170 \times 10^{-6}$ ,  $-90 \times 10^{-6}$ , and  $-100 \times 10^{-6}$ , respectively.

### The Crystallographic Structure and Geometry of $U^{4+}$ Ion Coordination in Uranium Sulfates

The basic parameters of the crystallographic structures of the uranium sulfates under consideration are presented in Table I.

The crystal of  $U(SO_4)_2 \cdot 4H_2O$  is built up of layers parallel to the *yz* plane and formed by uranium ions and sulfate groups. The layers are held together by water molecules via hydrogen bonds. Because of the arrangement

TABLE I  
 CRYSTAL STRUCTURE PARAMETERS OF  $U^{4+}$  SULFATES

Compound	Crystal system space group	Lattice constants (Å)	Number of U ions in unit cell	Minimum U-U distance (Å)	Average U-O distance in antiprism (Å)	Volume per U ion (Å <sup>3</sup> /U)
$U(SO_4)_2 \cdot 4H_2O$	Orthorhombic $D_{2h}^{16}-Pnma$	$a = 14.674$ $b = 11.093$ $c = 5.688$	4	6.50	2.40	232
$U_5O_4(OH)_4(SO_4)_6$	Tetragonal $C_{4h}^3-I4/m$	$a = 10.741$ $c = 10.377$	12	3.85 (4.98)	2.37	100
$U(OH)_2SO_4$	Orthorhombic $D_{2h}^{16}-Pnma$	$a = 11.572$ $b = 5.926$ $c = 6.969$	4	3.90 (5.96)	2.37	120

of the uranium positions, the lattice is magnetically diluted (232 Å<sup>3</sup>/U). The shortest U-U distances within the layer and between the adjacent layers approximate one another and are 6.55 and 6.50 Å, respectively. Every uranium ion is in contact with four sulfate groups and four water molecules, so that the eight oxygen anions coordinated around the uranium form a square Archimedean antiprism (Fig. 1). The eightfold inversion axes 8 of all the coordination antiprisms have a common z-axis direction. A certain distortion of the coordination polyhedron of the uranium, noticeable in Figs. 1a and b, is rather slight.

However, it should be mentioned that because of difficulty in determining the oxygen parameters, they may be in error by 0.01 of the lattice constants (a few tenths of angstroms), which means that the distortion is comparable to the error in the oxygen atom positions. The U-O distance within the antiprism ranges from 2.36 to 2.43 Å, assuming somewhat smaller values for oxygens of the hydration water molecules. The *trans* square of the antiprism (upper square in Fig. 1) is not exactly plane and is a little smaller than the lower *cis* square, which in turn is flat, but out of the *xy* plane. The average ratio of the height

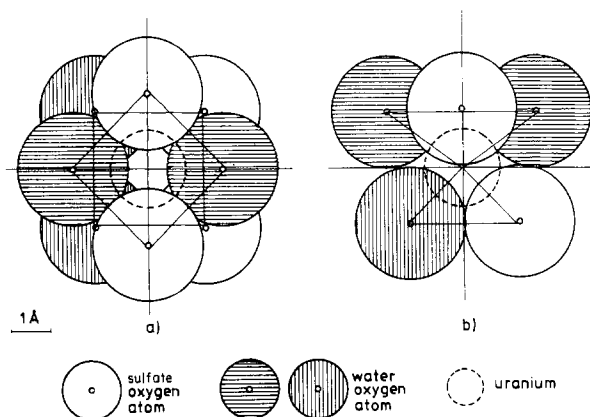


FIG. 1. Coordination of  $U^{4+}$  ion in  $U(SO_4)_2 \cdot 4H_2O$  (to scale). (a) Projection on the *xy* plane. (b) Projection on the *xz* plane. The projections of the square Archimedean antiprism for the oxygen radius 1.39 Å are drawn with solid lines.

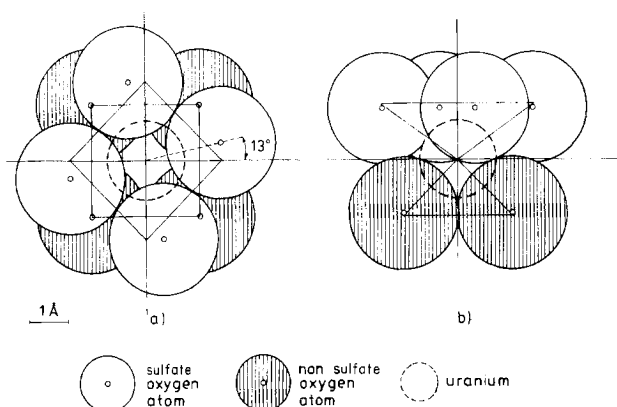


FIG. 2. Coordination of  $U^{4+}$  ion in  $U_6O_4(OH)_4(SO_4)_6$  (to scale). (a) Projection on the  $xy$  plane. (b) Projection on the  $xz$  plane ( $x$  and  $y$  axes of the antiprism are rotated in relation to the crystallographic axes by  $6.9^\circ$  around the  $z$  axis). The projections of the square Archimedean antiprism for the oxygen radius  $1.39 \text{ \AA}$  are drawn with solid lines.

of the antiprism to its edge of the square ( $c/a$ ) is equal to 1.01.

$U_6O_4(OH)_4(SO_4)_6$  has a body-centered tetragonal cell and a rather unusual arrangement of the metal ions, differing greatly from the structures of the two other sulfates. The structure is built up of sulfate ions and separate  $[U_6O_4(OH)_4]^{12+}$  octahedral groups with a U–U distance of  $3.85 \text{ \AA}$ . The shortest U–U distance between the two uranium octahedra is considerably longer ( $4.98 \text{ \AA}$ ). Every octahedron is surrounded by four oxy and four hydroxy ions forming a cube. The groups are joined in the crystal by sulfate ions, so that the coordination of oxygen anions around uranium is eightfold in a shape resembling a square Archimedean antiprism (Fig. 2). The  $\bar{8}$  axes of all the coordination antiprisms have a common  $z$ -axis direction. Both oxygen squares are perfectly flat, but the angle between them is only  $32^\circ$ , which is considerably less than  $45^\circ$ —the value for the ideal antiprism. Therefore, this is the case of “twisted cube” coordination ( $D_4$ ), which is more general than that of antiprismatic coordination ( $D_{4d}$ ). The polyhedron is flattened, and the  $c/a$  ratio is equal to 0.93. All eight U–O distances within the antiprism are practically the same ( $2.37 \text{ \AA}$ ). There is no information about the arrangement of the  $O^{2-}$  and  $OH^-$  ions within one of

the two square bases of the coordination polyhedron.

Despite the fact that  $U(OH)_2SO_4$  belongs to the same space group as the tetrahydrate sulfate, it is distinguished by a peculiar lattice structure. The crystals of  $U(OH)_2SO_4$  are built up of zigzag  $[U(OH)_2]_n^{2n+}$ -chains running along the  $y$  axis. The chains are linked together by sulfate ions. The minimum U–U distance within the chain is  $3.90 \text{ \AA}$  (in  $UO_2$ ,  $3.87 \text{ \AA}$ ), whereas between adjacent chains it is as much as  $5.96 \text{ \AA}$ . Every uranium atom is surrounded by eight oxygen atoms—four from hydroxyl and four from sulfate anions, forming two nearly parallel, slightly distorted squares rotated against each other by  $45^\circ$  (Fig. 3). The  $\bar{8}$  axes of all the coordination antiprisms lie in the  $xz$  plane at an inclination angle of either  $+53.6^\circ$  or  $-53.6^\circ$  toward the  $z$  axis. This angle is constant for a given  $[U(OH)_2]_n^{2n+}$  thread but changes sign on going from one thread to the next. A distortion of the antiprism is shown in Fig. 3. The U–O distance varies from  $2.33$  to  $2.41 \text{ \AA}$ , assuming for hydroxyl oxygens (average  $2.34 \text{ \AA}$ ) somewhat lower values than those for sulfate oxygens (average  $2.39 \text{ \AA}$ ). The hydroxyl oxygens form a rectangle of side ratio 1.15 prolate along the  $y$  axis, and the tetragon of the sulphate oxygens (a bent deltoid prolate along the  $x$

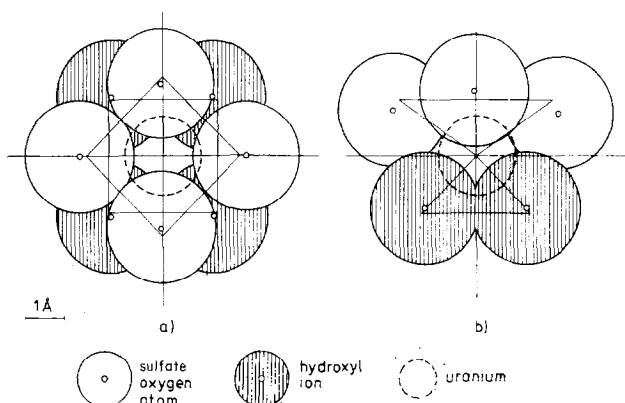


FIG. 3. Coordination of  $U^{4+}$  ion in  $U(OH)_2SO_4$  (to scale). (a) Projection on the  $xy$  plane ( $x$  and  $z$  axes of antiprism are rotated in relation to the crystallographic axes by  $\pm 53.6^\circ$  around the  $y$  axis). (b) Projection on the  $xz$  plane. The projections of the square Archimedean antiprism for the oxygen radius 1.39 Å are drawn with solid lines.

axis) is not perfectly flat. The antiprism is slightly flattened along the  $\bar{8}$  axis, with an average  $c/a$  ratio of 0.95.

### The Antiprismatic Crystal Field

The  $U^{4+}$  ion in the uranium sulfates is surrounded by eight oxygen anions which form an approximately square Archimedean antiprism. The electrostatic field of an antiprism symmetry is generated by eight identical point charges of coordinates:  $(a, a, c)$ ,  $(\bar{a}, \bar{a}, c)$ ,  $(\bar{a}, a, c)$ ,  $(a, \bar{a}, c)$ ,  $(a2^{1/2}, 0, \bar{c})$ ,  $(0, \bar{a}2^{1/2}, \bar{c})$ ,  $(\bar{a}2^{1/2}, 0, \bar{c})$ , and  $(0, a2^{1/2}, \bar{c})$ . For the Archimedean antiprism  $c/a = 1$ . The antiprism has  $\bar{8}2m-D_{4d}$  point group symmetry and the corresponding ligand field potential has an axial symmetry (4):

$$\begin{aligned} \mathcal{H}_{D_{4d}} = & \frac{Ze^2}{R^3} A_2^0 \alpha \langle r^2 \rangle \hat{O}_2^0 + \frac{Ze^2}{R^5} A_4^0 \beta \langle r^4 \rangle \hat{O}_4^0 \\ & + \frac{Ze^2}{R^7} A_6^0 \gamma \langle r^6 \rangle \hat{O}_6^0, \end{aligned} \quad (1)$$

where

$$\begin{aligned} A_2^0 &= 4 \frac{(c/a)^2 - 1}{(c/a)^2 + 2}, \\ A_4^0 &= \frac{1}{2} \frac{2(c/a)^4 - 12(c/a)^2 + 3}{[(c/a)^2 + 2]^2}, \\ A_6^0 &= \frac{1}{4} \frac{2(c/a)^6 - 30(c/a)^4 + 45(c/a)^2 - 5}{[(c/a)^2 + 2]^3}, \end{aligned} \quad (2)$$

$R = (2a^2 + c^2)^{1/2}$  is the central ion–ligand distance,  $\alpha$ ,  $\beta$ , and  $\gamma$  are the Stevens multiplicative factors,  $\langle r^n \rangle$  are the mean radii powers of the magnetic electrons, and  $\hat{O}_n^0$  are equivalent operators. The point group symmetry of the central ion and an axial character of the ligand field remain unchanged for any  $c/a$  ratio.

If the twisting angle of both square pyramids of the antiprism  $\alpha < 45^\circ$ , an octaverticon looks like a twisted cuboid and the tetragonal operators  $\hat{O}_4^4$  and  $\hat{O}_6^4$  with coefficients proportional to  $\cos 2\alpha$  occur in its electrostatic potential (4).

The ratio of ionic radii of  $U^{4+}$  ( $r = 0.97$  Å) and  $O^{2-}$  ( $R = 1.39$  Å) (5), amounting to  $r/R = 0.70$ , is not the optimum ratio for the cubic coordination (expected value  $\geq 0.73$ ). The uranium ion is somewhat small in relation to the hole in the center of the oxygen cube. Therefore the antiprismatic coordination is preferable in this case because of the possibility of some compression of the coordination polyhedron ( $c/a < 1$ ) and diminution of the hole reserved for the uranium ion (6). The optimum (contact) value of  $c/a$  depends on the ratio of the central ion and ligand radii according to the equation

$$(c/a)_{\text{opt}} = [(r/R)^2 + 2(r/R) - 1]^{1/2}. \quad (3)$$

For the ratio  $r/R = 0.70$ ,  $(c/a)_{\text{opt}} = 0.94$

### The Splitting of the ${}^3H_4$ Term in the $D_{4d}$ Crystal Field

In an antiprismatic crystal field the ninefold degenerate  ${}^3H_4$  term splits into four doublets,  $|\pm 4\rangle$ ,  $|\pm 3\rangle$ ,  $|\pm 2\rangle$ , and  $|\pm 1\rangle$ , and one singlet,  $|0\rangle$ . Theoretically, according to the values of the crystal field parameters, each of them can be the ground state. Calculations performed on the point charge model show that the doublets  $|\pm 3\rangle$  and  $|\pm 2\rangle$  are the ground levels for  $c/a$  values close to 1 ( $0.95 < c/a < 1.09$ ) and for smaller  $c/a$  values ( $0.92 < c/a < 0.95$ ) (4), respectively.

Low-symmetry distortions produce some splittings of the axial doublets  $|\pm M_J\rangle$  into two singlets, which in first approximation can be expressed as  $1/2^{1/2}|+M_J\rangle \pm 1/2^{1/2}|-M_J\rangle$ . Some admixtures of other wavefunctions to these singlets may be ignored because of their small amplitudes.

The splitting values  $\delta$  applied in the Van Vleck formula are not those of the point charge model, but they have been fitted empirically.

### The Paramagnetic Susceptibility of $U^{4+}$ Ion in the Antiprismatic Crystal Field

Interpretation of the temperature dependence of the magnetic susceptibility of the three uranium sulfates is based on the Van Vleck formula for a "limited" model taking into account only the two lowest axial doublets of the  ${}^3H_4$  term in the  $D_{4d}$  crystal fields,  $|\pm 2\rangle$

and  $|\pm 3\rangle$ , or alternatively, the four singlets originating in these doublets. The polarizing contributions to the susceptibility from higher excited levels are neglected in this approximation, although the assumption of their estimated values reduces the differences between the experimental and calculated values of the susceptibility, shifting simultaneously the energy of the excited levels upward. This is illustrated by an example of  $\chi(T)$  dependence for  $U(SO_4)_2 \cdot 4H_2O$  and  $U(OH)_2SO_4$ . The low- and high-frequency components of the paramagnetic susceptibility of the  $U^{4+}$  ion eigenstates in the  $D_{4d}$  crystal field are listed in Table II.

Owing to the axial symmetry of the effective crystal field potential, the magnetic susceptibility of the  $U^{4+}$  ion shows an anisotropy. All expressions for magnetic susceptibility given below refer to its average value for axial anisotropy:

$$\chi = \frac{1}{3}(\chi^{\parallel} + 2\chi^{\perp}),$$

where  $\chi^{\parallel}$  denotes the susceptibility along the  $\bar{8}$  axis and  $\chi^{\perp}$  the susceptibility in the direction perpendicular to it.

In the case of a low-symmetry distortion and a splitting of the axial doublet  $|\pm M_J\rangle$  into the two singlets  $1/2^{1/2}|+M_J\rangle \pm 1/2^{1/2}|-M_J\rangle$ , the term of the susceptibility corresponding to their mutual high-frequency interaction amounts to  $\chi_{hf} = 0.16 M_J^2/\delta$ , where  $\delta$  is the distance, in degrees Kelvin, between them. The components of the susceptibility originating in

TABLE II  
LOW- AND HIGH-FREQUENCY COMPONENTS OF PARAMAGNETIC SUSCEPTIBILITY OF  
 $U^{4+}$  ION IN  $D_{4d}$  CRYSTAL FIELD

$ M_J\rangle$	$ 0\rangle$	$ \pm 1\rangle$	$ \pm 2\rangle$	$ \pm 3\rangle$	$ \pm 4\rangle$
$ 0\rangle$	0	$3.20/\delta_{01}$	0	0	0
$ \pm 1\rangle$	—	$0.16/T$	$2.88/\delta_{12}$	0	0
$ \pm 2\rangle$	—	—	$0.64/T$	$2.24/\delta_{23}$	0
$ \pm 3\rangle$	—	—	—	$1.44/T$	$1.28/\delta_{34}$
$ \pm 4\rangle$	—	—	—	—	$2.56/T$

$\delta_{ij}$  denotes the energy gap between  $|\pm i\rangle$  and  $|\pm j\rangle$  doublets in degrees Kelvin.

the interactions between either symmetrical or antisymmetrical singlets  $|1/2^{1/2} + M_J\rangle \pm |1/2^{1/2} - M_J\rangle$  and  $|1/2^{1/2} + M_J \pm 1\rangle \pm |1/2^{1/2} - M_J \mp 1\rangle$  are equal to one-half of the components for the corresponding  $|\pm M_J\rangle$  and  $|\pm (M_J \pm 1)\rangle$  doublets.

### Results and Discussion

The temperature dependence of the paramagnetic susceptibility of  $U(SO_4)_2 \cdot 4H_2O$  is shown in Fig. 4. The susceptibility at 4.2°K amounts to  $10820 \times 10^{-6}$  and may be regarded as temperature independent up to ca. 50°K, after which it falls regularly with temperature, attaining the value of  $3790 \times 10^{-6}$  at room temperature (294°K). The temperature dependence of the susceptibility

over the entire temperature range can be described by the expression

$$\begin{aligned} \chi = & \left[ \left( \frac{1.44}{\delta_1} + \frac{1.12}{\delta_3} \right) + \left( -\frac{1.44}{\delta_1} + \frac{1.12}{\delta_2 - \delta_1} \right) \right. \\ & \times \exp\left(-\frac{\delta_1}{T}\right) + \left( \frac{0.64}{\delta_3 - \delta_2} - \frac{1.12}{\delta_2 - \delta_1} \right) \\ & \times \exp\left(-\frac{\delta_2}{T}\right) + \left( -\frac{0.64}{\delta_3 - \delta_2} - \frac{1.12}{\delta_3} \right) \\ & \times \exp\left(-\frac{\delta_3}{T}\right) \left. \right] \times \left[ 1 + \exp\left(-\frac{\delta_1}{T}\right) \right. \\ & \left. + \exp\left(-\frac{\delta_2}{T}\right) + \exp\left(-\frac{\delta_3}{T}\right) \right]^{-1}, \quad (4) \end{aligned}$$

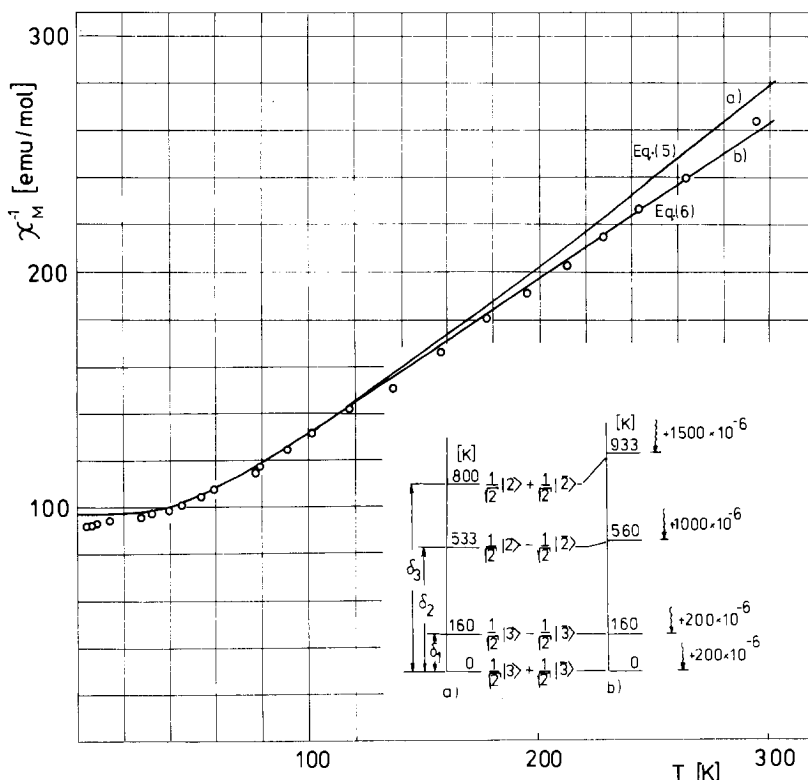


FIG. 4. Reciprocal molar susceptibility of  $U(SO_4)_2 \cdot 4H_2O$  vs temperature within the range 4.2–300°K. O, Experimental points; solid lines, theoretical according to Eqs. (5) and (6) and splitting diagrams (a) and (b).

where  $\delta_1 = 160^\circ\text{K}$ ,  $\delta_2 = 533^\circ\text{K}$ , and  $\delta_3 = 800^\circ\text{K}$ . Thus,

$$\chi = \left[ 0.010400 - 0.006000 \exp\left(-\frac{160}{T}\right) - 0.000600 \exp\left(-\frac{533}{T}\right) - 0.003800 \exp\left(-\frac{800}{T}\right) \right] \times \left[ 1 + \exp\left(-\frac{160}{T}\right) + \exp\left(-\frac{533}{T}\right) + \exp\left(-\frac{800}{T}\right) \right]^{-1} \quad (5)$$

higher excited levels. An estimation of these contributions, as, for instance, in Fig. 4b, modifies somewhat the splitting diagram and leads to an expression similar to Eq. (5):

$$\chi = \left[ 0.010400 - 0.00600 \exp\left(-\frac{160}{T}\right) - 0.001500 \exp\left(-\frac{933}{T}\right) \right] \times \left[ 1 + \exp\left(-\frac{160}{T}\right) + \exp\left(-\frac{560}{T}\right) + \exp\left(-\frac{933}{T}\right) \right]^{-1} \quad (6)$$

This is the model dependence neglecting the polarizing contributions coming from the

(5) A certain rise in energy of the excited levels is noticeable. The ground state of the  $\text{U}^{4+}$  ion in  $\text{U}(\text{SO}_4)_2 \cdot 4\text{H}_2\text{O}$  consists of two singlets  $|1/2^{1/2}|3\rangle \pm |1/2^{1/2}|-3\rangle$  separated by  $160^\circ\text{K}$ .

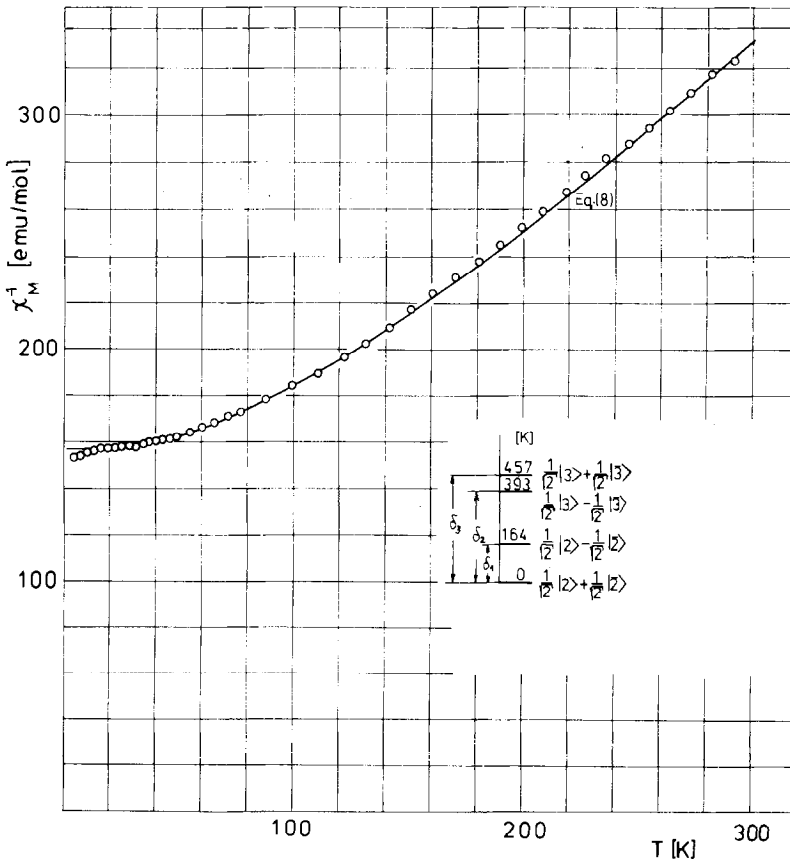


FIG. 5. Reciprocal molar susceptibility of  $\text{U}_6\text{O}_4(\text{OH})_4(\text{SO}_4)_6$  vs temperature within the range 4.2–300°K. O, Experimental points; solid line, theoretical according to Eq. (8) and splitting diagram presented.



Assuming an undisturbed antiprismatic pattern of levels, i.e., assuming that the energy gap between the  $| \pm 3 \rangle$  and  $| \pm 2 \rangle$  doublets is equal to 0.3 of the total splitting of the  $^3H_4$  term, one may estimate the latter to be ca. 2300°K (1600 cm<sup>-1</sup>). However, because of the simplifying assumptions mentioned above, this value should be treated as approximate.

The temperature dependence of the paramagnetic susceptibility of U<sub>6</sub>O<sub>4</sub>(OH)<sub>4</sub>(SO<sub>4</sub>)<sub>6</sub> is presented in Fig. 5. The susceptibility is roughly temperature independent in the range up to 50°K, where it amounts to  $6400 \times 10^{-6}$ . Then, the susceptibility drops with temperature attaining  $3090 \times 10^{-6}$  at room temperature (292.5°K). Over the entire temperature range up to 300°K the dependence may be correctly described by the

model expression according to the splitting diagram given in Fig. 5:

$$\chi = \left[ \left( \frac{0.64}{\delta_1} + \frac{1.12}{\delta_3} \right) + \left( -\frac{0.64}{\delta_1} + \frac{1.12}{\delta_2 - \delta_1} \right) \times \exp \left( -\frac{\delta_1}{T} \right) + \left( \frac{1.44}{\delta_3 - \delta_2} - \frac{1.12}{\delta_2 - \delta_1} \right) \times \exp \left( -\frac{\delta_2}{T} \right) + \left( -\frac{1.44}{\delta_3 - \delta_2} - \frac{1.12}{\delta_3} \right) \times \exp \left( -\frac{\delta_3}{T} \right) \right] \times \left[ 1 + \exp \left( -\frac{\delta_1}{T} \right) + \exp \left( -\frac{\delta_2}{T} \right) + \exp \left( -\frac{\delta_3}{T} \right) \right]^{-1}, \quad (7)$$

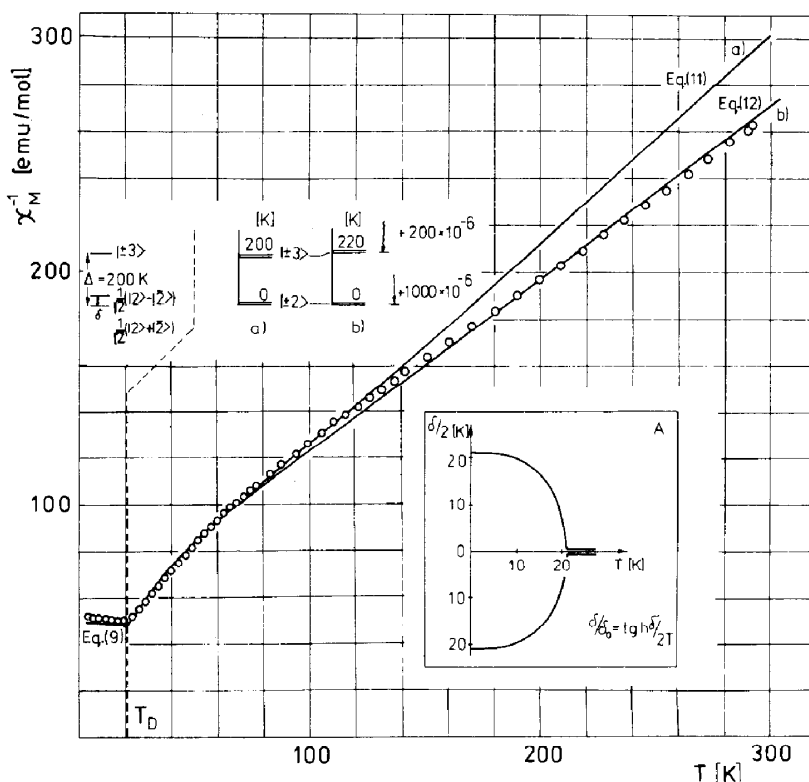


FIG. 6. Reciprocal molar susceptibility of U(OH)<sub>2</sub>SO<sub>4</sub> vs temperature within the range 4.2–300°K. O, Experimental points; solid lines, theoretical according to Eqs. (11) and (12) for splitting diagrams (a) and (b), respectively, above T<sub>D</sub>, and the theoretical plot according to Eq. (9) for the splitting diagram below T<sub>D</sub>. Inset A: the course of  $\delta(T)$  below T<sub>D</sub>.

where  $\delta_1 = 164^\circ\text{K}$ ,  $\delta_2 = 393^\circ\text{K}$ , and  $\delta_3 = 457^\circ\text{K}$ . Equation (7) is then

$$\chi = \left[ 0.006350 - 0.001000 \exp\left(-\frac{164}{T}\right) + 0.017600 \exp\left(-\frac{393}{T}\right) - 0.024950 \exp\left(-\frac{457}{T}\right) \right] \times \left[ 1 + \exp\left(-\frac{164}{T}\right) + \exp\left(-\frac{393}{T}\right) + \exp\left(-\frac{457}{T}\right) \right]^{-1} \quad (8)$$

This means that the  $U^{4+}$  ground state in this compound is composed of two singlets  $|1/2^{1/2}|2\rangle \pm |1/2^{1/2}|-2\rangle$  separated from each other by  $164^\circ\text{K}$ . One may notice the inverse sequence of the symmetrical and antisymmetrical singlets originating in the axial doublets  $|\pm 2\rangle$  and  $|\pm 3\rangle$  in both  $U(\text{SO}_4)_2 \cdot 4\text{H}_2\text{O}$  and  $U_6\text{O}_4(\text{OH})_4(\text{SO}_4)_6$  sulfates. The model description allows this sequence to be determined unambiguously.

The dependence of the magnetic susceptibility of  $U(\text{OH})_2\text{SO}_4$  vs temperature, as measured by the Faraday method, is presented in Fig. 6. Within the temperature range  $4.2\text{--}21^\circ\text{K}$  ( $=T_D$ ) the susceptibility is roughly constant, displaying, however, a slight increase from  $19040 \times 10^{-6}$  at  $4.2^\circ\text{K}$  to  $19880 \times 10^{-6}$  at  $21^\circ\text{K}$ . At  $21^\circ\text{K}$  a sudden change in the character of the  $\chi(T)$  dependence takes place. Above this temperature the susceptibility decreases if the dependence is typical for a paramagnet with a degenerate ground state. At room temperature ( $292^\circ\text{K}$ ) the susceptibility reaches the value of  $3800 \times 10^{-6}$ . In the range below  $21^\circ\text{K}$  the susceptibility obeys the equation

$$\chi = \left[ \left( \frac{0.64}{\delta} + \frac{1.12}{200 + \frac{\delta}{2}} \right) + \left( -\frac{0.64}{\delta} + \frac{1.12}{200 - \frac{\delta}{2}} \right) \right] \times \exp\left(-\frac{\delta}{T}\right) \left[ 1 + \exp\left(-\frac{\delta}{T}\right) \right]^{-1} \quad (9)$$

in which  $\delta$  varies with  $T$  according to the relation (Fig. 6A)

$$\frac{\delta}{\delta_0} = \text{tgh} \frac{\delta T_D}{\delta_0 T} \quad (10)$$

where  $\delta_0 = 2T_D = 42^\circ\text{K}$  is the value of  $\delta$  at  $0^\circ\text{K}$ . Equation (9) explains the increase of the susceptibility by ca.  $600 \times 10^{-6}$  observed experimentally in the range  $4.2\text{--}21^\circ\text{K}$ .

Above  $21^\circ\text{K}$  the susceptibility follows the equation

$$\chi = \left[ \left( \frac{0.64}{T} + \frac{2.24}{200} \right) + \left( \frac{1.44}{T} - \frac{2.24}{200} \right) \times \exp\left(-\frac{200}{T}\right) \right] \left[ 2 + 2 \exp\left(-\frac{200}{T}\right) \right]^{-1} \quad (11)$$

An estimated contribution of the polarizing terms from the upper levels modifies the splitting diagram to a certain degree (Fig. 6b) and leads to the equation

$$\chi = \left[ \left( \frac{0.64}{T} + 0.011200 \right) + \left( \frac{1.44}{T} - 0.009800 \right) \times \exp\left(-\frac{220}{T}\right) \right] \left[ 2 + 2 \exp\left(-\frac{220}{T}\right) \right]^{-1} \quad (12)$$

which fits the experimental points better. From Eqs. (9) and (11) it follows that above  $21^\circ\text{K}$  the doublet  $|\pm 2\rangle$  is the electronic ground state of the  $U^{4+}$  ion and the next  $|\pm 3\rangle$  doublet about  $200^\circ\text{K}$  distant is the first excited level. Since verification of this model is possible only above  $21^\circ\text{K}$ , the occurrence of some slight "zero" splittings of the doublets caused by deviations from the axially of the crystal field cannot be excluded, and consequently they are neglected. The behavior of the  $\chi(T)$  dependence below  $21^\circ\text{K}$  is very distinctive and may be explained by a distortion of the axial crystal field due to a crystallographic transition induced by the cooperative Jahn-

Teller effect. A result of the distortion is that the ground state of the U<sup>4+</sup> ion below  $T_D$  is the system of two singlets  $1/2^{1/2}|2\rangle \pm 1/2^{1/2}|-2\rangle$  separated by  $\delta(T)$ .

Magnetic measurements performed by the vibrating-sample magnetometer at 4.2°K yielded a linear dependence of the magnetization on the magnetic field intensity over the entire range of the applied magnetic field from 0 to 50 kOe. In addition, a slight decrease in  $T_D$  (ca. 1°K) with an increase of the magnetic field from 5 to 50 kOe was observed.

The fairly large differences in the magnetic behavior of the three uranium sulfates at low temperatures are clearly visible. They occur despite the fact that the differences in the U<sup>4+</sup> ion surroundings are rather subtle. At 4.2°K the susceptibility of U(OH)<sub>2</sub>SO<sub>4</sub> is almost twice as large as the susceptibility of U(SO<sub>4</sub>)<sub>2</sub>·4H<sub>2</sub>O and three times that of U<sub>6</sub>O<sub>4</sub>(OH)<sub>4</sub>(SO<sub>4</sub>)<sub>6</sub>. It proves the essential influence of the surroundings on the magnetic properties of the U<sup>4+</sup> ion.

Neglecting some discrepancies between the experimental and calculated  $\chi(T)$  plots observed at higher temperatures, the qualitative consistency with the assumed model of the antiprismatic crystal field is beyond doubt. The agreement between the experimental values of the susceptibility and the values calculated according to Van Vleck's formula for such a simplified model is even more striking in the light of previously obtained results such as, for example, those reported in Refs. (7–8). On the other hand, one should not regard the estimated energy values (with the accuracy given in the equations and diagrams) as the actual values. They undergo changes when the exact compositions of the eigenfunctions and the polarizing contributions of the upper levels are taken into consideration rigorously, especially for the excited levels. The estimation of the polarizing contributions in both U<sub>6</sub>O<sub>4</sub>(OH)<sub>4</sub>(SO<sub>4</sub>)<sub>6</sub> and U(OH)<sub>2</sub>SO<sub>4</sub> is still more uncertain because the pattern of levels, owing to the  $c/a$  ratio, does not correspond to that established for the perfect square antiprism and the splitting, owing to a

somewhat shorter U–O distance, seems to be stronger than that for U(SO<sub>4</sub>)<sub>2</sub>·4H<sub>2</sub>O.

None of the uranium sulfates considered above has the purely antiprismatic coordination of the uranium ion. However, the deviations from the axially of the crystal field do not destroy the axial character of the splitting diagrams of the <sup>3</sup>H<sub>4</sub> term. Only for U(SO<sub>4</sub>)<sub>2</sub>·4H<sub>2</sub>O is the average  $c/a$  ratio of the coordination antiprism close to 1, whereas for the remaining two sulfates it is close to 0.94—the optimum value expected for the ratio of the U<sup>4+</sup> and O<sup>2-</sup> ion radii (0.70). According to the point charge model the ground state in the first case originates in the  $|\pm 3\rangle$  doublet; in other cases ( $c/a \approx 0.94$ ), in the  $|\pm 2\rangle$  doublet. The splittings of the ground doublets in U(SO<sub>4</sub>)<sub>2</sub>·4H<sub>2</sub>O and U<sub>6</sub>O<sub>4</sub>(OH)<sub>4</sub>(SO<sub>4</sub>)<sub>6</sub> are roughly the same, amounting to ca. 160°K (115 cm<sup>-1</sup>). In U(OH)<sub>2</sub>SO<sub>4</sub> the ground doublet  $|\pm 2\rangle$  is practically unsplit above 21°K, but below, the cooperative Jahn–Teller effect is presumably observed.

In the crystal lattice of U(SO<sub>4</sub>)<sub>2</sub>·4H<sub>2</sub>O, which is slightly less compact than those of the two remaining alkaline uranium sulfates, the coordination polyhedron is very close to the ideal Archimedean antiprism (Fig. 1). The deviations from the axially of the ligand field are presumably induced in this case by the lack of a center of inversion within one of the square bases of an antiprism (*cis* square, lower in Fig. 1) resulting from the nonequivalence of oxygen ligands originating in water molecules and sulfate groups.

U<sub>6</sub>O<sub>4</sub>(OH)<sub>4</sub>(SO<sub>4</sub>)<sub>6</sub> would probably have the purest axial ligand field where it not for the fact that both antiprisms' pyramids are twisted with respect to each other, not by 45°, but only by 32° (Fig. 2). The contribution of the tetragonal terms in the electrostatic potentials of such polyhedra amounts to about 0.4 of the contribution in the cubic field ( $\cos 64^\circ \approx 0.44$ ). This fact explains the appreciable splitting of the ground  $|\pm 2\rangle$  doublet.

For U(OH)<sub>2</sub>SO<sub>4</sub>, despite the fact that the coordination polyhedron (Fig. 3) shows some

geometrical differences in relation to the ideal antiprism, the electrostatic ligand field (above 21°K) has an axial character.

The three uranium sulfates are paramagnets over the entire temperature range. Only  $U(OH)_2SO_4$  shows the cooperative Jahn–Teller effect below 21°K. The lack of a magnetic ordering is due to the considerable magnetic dilution of the crystal lattices (Table 1) and to the “island” or “thready” structure of the uranium ion sublattice occurring in  $U_6O_4(OH)_4(SO_4)_6$  and  $U(OH)_2SO_4$ , respectively. The lattice volume per uranium ion may be some measure of this dilution. For the sulfates it varies from 100 to 232 Å<sup>3</sup>/U, whereas for  $UO_2$  it is equal to only 41 Å<sup>3</sup>/U.

The cooperative Jahn–Teller effect discovered in  $U(OH)_2SO_4$  is the first case of this kind found in the actinide compounds. So far, it has been reported for a number of tetragonal vanadates (9–11), arsenates (12), and phosphates (13) of the trivalent rare earths at low temperatures. The  $\delta(T)$  dependence (Eq. (10)) on the ground singlet of the molecular field approximation derived under the assumption that the strain energy is proportional to  $\delta^2$  gives, neglecting high-frequency terms, a constant value of the susceptibility below  $T_D$  of  $0.64/2T_D$ . The high-frequency term of the ground singlet, neglecting a possible splitting of the excited  $|\pm 3\rangle$  doublet, is equal to  $1.12/(200 + \delta/2)$ . When the temperature rises from 4.2 to 21°K, this term increases and attains the value  $1.12/200$  at 21°K. The predicted increase of the susceptibility ( $600 \times 10^{-6}$ ) corresponds roughly to that observed experimentally ( $600\text{--}800 \times 10^{-6}$ ). The tendency of  $T_D$  to decrease (broadening of the undistorted phase range) with an increase in magnetic field intensity is presumably due to the fact that the Zeeman splitting of the degenerate  $|\pm 2\rangle$  doublet may (for small  $\delta$ ) give a ground state energy in the undistorted phase lower than the splitting produced by the crystalline distortion.

The physical origin of the cooperative Jahn–Teller effect in  $U(OH)_2SO_4$  is not yet known. Apart from the electron–phonon

coupling it may be electric quadrupole–quadrupole or other multipole–multipole interactions. The most effective Jahn–Teller loss of energy of the electronic ground doublet  $|\pm 2\rangle$  would be caused by such a crystallographic distortion, which would produce the tetragonal terms of the ligand field potential at the uranium site. To a large extent it would correspond either to the electrostatic imbalance between both squares of an antiprism or to their common twist.

Still unknown are the crystallographic structure of the low-temperature phase and the type of distortion, as well as the temperature dependence of the heat capacity of  $U(OH)_2SO_4$ . These will be the subjects of a future work. The predicted energy  $U$  associated with the specific heat anomaly is  $\delta_0 R/4 \approx 21$  cal/mole.

#### Acknowledgment

I would like to thank Z. Żolnierek for suggesting the cooperative Jahn–Teller nature of the magnetic anomaly in  $U(OH)_2SO_4$  at 21°K.

#### References

1. G. LUNDGREN, *Ark. Kemi* **4**, 421 (1952).
2. G. LUNDGREN, *Ark. Kemi* **5**, 349 (1953).
3. P. KIERKEGAARD, *Chem. Scand.* **10**, 599 (1956).
4. J. MULAK AND A. CZOPNIK, *Bull. Acad. Polon. Sci., Ser. Sci. Chim.* **20**, 209 (1972).
5. R. S. C. WYCKOFF, “Crystal Structures,” Interscience, New York (1958).
6. L. PAULING, “The Nature of the Chemical Bond,” 2nd ed., p. 382, Cornell Univ. Press, New York (1940).
7. C. A. HUTCHISON AND G. A. CANDELA, *J. Chem. Phys.* **27**, 707 (1957).
8. R. A. SATTEN, C. L. SCHREIBER, AND E. Y. WONG, *J. Chem. Phys.* **42**, 162 (1965).
9. A. H. COOKE, C. J. ELLIS, K. A. GEHRING, M. J. M. LEASK, D. M. MARTIN, B. M. WANKLYN, M. R. WELLS, AND R. L. WHITE, *Solid State Commun.* **8**, 689 (1970).
10. K. A. GEHRING, A. P. MALOZEMOFF, W. STAUDE, AND R. N. TYTE, *Solid State Commun.* **9**, 511 (1971).
11. A. H. COOKE, S. J. SWITENBY, AND M. R. WELLS, *Solid State Commun.* **10**, 265 (1972).
12. L. KLEIN, W. WÜCHNER, H. G. KAHLE, AND H. C. SCHOPPER, *Phys. Status Solidi B* **48**, K139 (1971).
13. J. F. L. LEWIS AND G. A. PRINZ, *Phys. Rev. B* **10**, 2892 (1974).